

論文 / 著書情報  
Article / Book Information

論題(和文)	
Title(English)	Performance Evaluation of Wireless Sensor Network Based on MIMO Relaying Channel Capacity
著者(和文)	KYLENG, 阪口啓, 荒木純道
Authors(English)	Leng KY, Kei Sakaguchi, Kiyomichi Araki
出典(和文)	, Vol. E92-B, No. 10, pp. 3166-3173
Citation(English)	IEICE Transaction on Communications, Vol. E92-B, No. 10, pp. 3166-3173
発行日 / Pub. date	2009, 10
URL	<a href="http://search.ieice.org/">http://search.ieice.org/</a>
権利情報 / Copyright	本著作物の著作権は電子情報通信学会に帰属します。 Copyright (c) 2009 Institute of Electronics, Information and Communication Engineers.

## PAPER

# Performance Evaluation of Wireless Sensor Network Based on MIMO Relaying Channel Capacity

KY LENG<sup>†a)</sup>, *Nonmember*, Kei SAKAGUCHI<sup>†</sup>, *Member*, and Kiyomichi ARAKI<sup>†</sup>, *Fellow*

**SUMMARY** In this paper, the performance of the Wireless Sensor Network (WSN) using fixed relay nodes and Multiple-Input Multiple-Output (MIMO) technology was evaluated based on the correlated channel capacity of MIMO system and the number of sensor node served by the system. Moreover, the performance evaluation of the proposed algorithm, which is used to find the optimum distance to place the relay nodes from sink node, is done not only with AF relaying and spatial correlation effect, but also with Decode-and-Forward (DF) relaying scheme. The results show that the relay gain (a ratio between the maximum number of sensors satisfying the required channel capacity in 7-cell topology to the number of sensor nodes in sink cell) is affected strongly by the spatial correlation at high required channel capacity but little at low required channel capacity. The results also show that the relay gain can be improved remarkably by using the DF relaying scheme, and that the validity of the proposed algorithm holds for any relaying scheme, spatial correlation effect and different antenna size.

**key words:** WSN, MIMO relay network, relay position, AF, DF, spatial correlation

## 1. Introduction

Multiple-Input Multiple-Output (MIMO) technology has attracted attention in wireless communications, since it offers significant increases in data throughput and link range without additional bandwidth or transmitted power [1]. In addition, the integration of MIMO technology into Wireless Sensor Network (WSN) offers some benefit over the conventional WSN. Accordingly, this paper evaluates the capacity of a WSN that uses the MIMO technique.

The works in [2]–[7] are different from ours in many aspects. Basically, when MIMO system simulations are performed, the propagation channels are assumed independent of each other i.e. I.I.D Rayleigh fading channel. In reality, the signals received by different receiver antennas are correlated with each other in space, time and spectrum [8], [9]. Since these correlations are assumed independent [9], and that in WSN, all sensor nodes are assumed to be fixed (no temporal correlation) and the propagation channel is narrowband (no spectral correlation), we take into consideration only the spatial correlation effect.

The MIMO channel capacity is severely degraded by the spatial correlation factor [8], [9], and that the performance of Decode-and-Forward (DF) scheme is better than the AF scheme in some conditions only [10]. So, it is important to check the following questions:

- Does the spatial correlation have influence on optimum relay position (position where the network can guarantee a minimum channel capacity to the largest number of sensor nodes)?
- Is the proposed algorithm to find this optimum relay position still valid under the influence of spatial correlation?
- Can relay gain be improved by using the DF relaying scheme?
- Is the proposed algorithm to find this optimum relay position still valid under the DF relaying scheme and spatial correlation influence?
- Is the proposed algorithm still valid for different antenna size (let say  $2 \times 2$  MIMO or SISO)?

The rest of this paper is organized as follows. Section 2 points out the problem/objective of the design and the algorithms which are used to solve that problem. Section 3 describes the MIMO channel model with spatial correlation. Section 4 derives the formulas for the MIMO channel capacity in the relay network for both AF and DF, and the simplified version of the predictor using Jensen's inequality is proposed in Sect. 5. The performances of the proposed algorithm are discussed in Sect. 6. Finally, the conclusion is presented in Sect. 7.

## 2. Problem and Algorithms

**Problem:** Given a set of sensor nodes which is uniformly distributed in a plane, and a minimum required channel capacity  $C_{lim}$ ; find the optimal relay distance  $R = \mathcal{R} = \sqrt{3}r$ , where  $r$  is the radius of the cell and  $\mathcal{R}$  is the Sink-Relay distance, that can cover the largest number of sensor nodes in 7 cells topology. For simplification, we take  $r \in [0, 2r_{max}]$  in the simulation ( $r_{max}$  is calculated from the link budget with signal-to-noise ratio  $SNR = 0$  dB at the receiver).

The algorithms below are proposed to solve the problem above.

### Exhaustive search:

1. In order to guarantee the uniformity of the sensor in the field throughout different coverage areas, we generate the locations of sensor nodes in a square plane (we generate  $2 \times 10^5$  sensor nodes in  $5569 \times 5569$  m<sup>2</sup> square plane).
2. Find  $r_{max}$  from roof-to-ground (RG) pathloss model and link budget.
3. For a given value of  $r$  (radius of a cell varies from 0

Manuscript received February 17, 2009.

Manuscript revised June 15, 2009.

<sup>†</sup>The authors are with the Tokyo Institute of Technology, Tokyo, 152-8552 Japan.

a) E-mail: leng@mobile.ee.titech.ac.jp

DOI: 10.1587/transcom.E92.B.3166

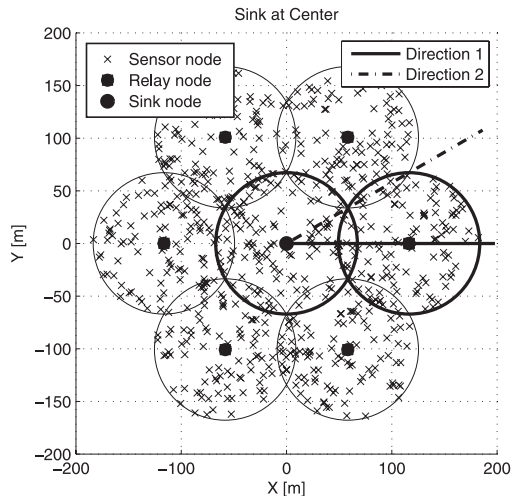


Fig. 1 Direction of cross-point or sensor node.

to  $2r_{max}$ ), calculate the relay distance from sink node  $\mathcal{R} = \sqrt{3}r$  as well as the location of 6 surrounding relay nodes. See also Fig. 1.

4. Calculate the channel capacity  $C_i$  of all sensor nodes in the coverage of 7-cells topology. If the sensor is in the coverage of the sink cell, Eq. (11) will be used ( $C_i = C_{Direct}$ ) and if the sensor is out of the sink cell but in the coverage of other 6 surrounding cells, Eq. (13) or Eq. (19) will be used ( $C_i = C_{Relay}$ ) depending on the relay scheme.
5. Count the number of sensor nodes which have  $C_i \geq C_{lim}$ . Repeat from step 3 until  $r = 2r_{max}$ .
6. Extract the number of sensor nodes that have  $C_i \geq C_{lim}$  in the sink cell.
7. Repeat from step 1 for different value of  $C_{lim}$ .

**Proposed Algorithm:** We consider the channel capacity at the cross-point ( $C_{Direct} = C_{Relay}$ ) as the minimum required capacity  $C_{lim}$ , and the position of the relay node that satisfies this condition as the optimum relay position  $\mathcal{R}$ . By considering the hexagonal alignment (7-cell topology) as an optimal topology for the WSN, we proposed two algorithms according to the distribution of the sensor nodes with respect to the direction of sink-relay node. One considers this distribution on the same direction of sink-relay (called MonteCarlo-D1) which corresponds to a maximum 7-cell-edge distance, and the other method considers a direction shifted  $30^\circ$  from the first one (called MonteCarlo-D2) which corresponds to a minimum 7-cell-edge distance. See also Fig. 1 for the optimization direction and 7-cell topology. The corresponding Jensen's inequality will be called Jensen-D1 and Jensen-D2 respectively.

The objective of this paper is to evaluate the validity of this method under the influence of spatial correlation and relay schemes. Note that the word optimum refers to the results from an exhaustive search. Normally, the exhaustive search is used to find the optimum position. However, since this method uses not only the exhaustive search within the

distributed sensor nodes in the field ( $2 \times 10^5$  sensor nodes in  $5569 \times 5569 \text{ m}^2$ ), but also requires Monte Carlo simulation, the computational load for this kind of method is huge. For this reason, MonteCarlo-D1 and MonteCarlo-D2 are proposed to reduce the heavy computation loads imposed by this exhaustive method.

### 3. MIMO Channel Model

Before starting our discussion, we state out some parameters used in this paper as follows:

- Four antennas for all nodes (sensors, relays, and sink)  $\Leftrightarrow 4 \times 4$  MIMO if not specified.
- $\frac{1}{2}\lambda$  antenna separation.
- 0 dBm total transmitted power for all nodes.
- Noise power at every node is assumed to be  $\sigma^2 = -100$  dBm.
- 0 dBi antenna gain for all nodes.
- Custom factory pathloss models in the frequency band of 950 MHz for Roof-to-Roof (RR), and Roof-to-Ground (RG) communication. Details are in [11].
- The sink node is located at the center of the six surrounding cells (Fig. 1).
- No collision occurs during transmission of each data frame.

Note that the frequency band of 950 MHz is allowed by Japanese Radio Law in April 2005 to be used by the Radio Frequency Identification (RFID) [12]. For this reason, our MIMO-WSN system will also work on this band.

Since the pathloss models are developed for a factory environment with a size of  $760 \times 1005 \text{ m}^2$  and that the result in [11] showed that the spatial correlation at both Tx and Rx is independent of antenna height and location, we can say that the channel model generated from these pathloss models can be separated into Tx side and Rx side, and that the direction of received signals at Rx are independent of that at Tx. Moreover, in real application, using four antennas at Tx and Rx side is more than enough for WSN application. By considering these factors, the proper correlation-based analytic model to be chosen for this environment is the Kronecker model.

Let  $\mathfrak{R}_{Tx}$  and  $\mathfrak{R}_{Rx}$  be the correlation matrix at Transmitter side (Tx) and Receiver side (Rx) respectively. So, the normalized Kronecker channel realizations can be generated by [13] as:

$$H = \mathfrak{R}_{Rx}^{\frac{1}{2}} U \mathfrak{R}_{Tx}^{\frac{1}{2}} \quad (1)$$

where  $U$  is a stochastic matrix with i.i.d. complex Gaussian zero-mean unit variance elements.

In this paper, we need only the spatial correlation for RR (Sink-Relay link) and RG (Relay-Sensor link). Since the main stream of data in WSN flow from sensor nodes to sink node through relay nodes, the reverse version of RG will be used (Ground-to-Roof). The final results of these correlation factors used in this paper are extended from [11]

as:

$$\mathfrak{R}_{T_{XS}}^{\frac{1}{2}} = \begin{bmatrix} 0.9426 & 0.1402 & 0.2473 & 0.1750 \\ 0.1402 & 0.9477 & 0.1450 & 0.2473 \\ 0.2473 & 0.1450 & 0.9477 & 0.1402 \\ 0.1750 & 0.2473 & 0.1402 & 0.9426 \end{bmatrix} \quad (2)$$

$$\mathfrak{R}_{R_{XR}}^{\frac{1}{2}} = \begin{bmatrix} 0.9412 & 0.1401 & 0.2530 & 0.1745 \\ 0.1401 & 0.9462 & 0.1450 & 0.2530 \\ 0.2530 & 0.1450 & 0.9462 & 0.1401 \\ 0.1745 & 0.2530 & 0.1401 & 0.9412 \end{bmatrix} \quad (3)$$

$$\mathfrak{R}_{T_{XR}}^{\frac{1}{2}} = \begin{bmatrix} 0.9430 & 0.1412 & 0.2611 & 0.1502 \\ 0.1412 & 0.9442 & 0.1426 & 0.2611 \\ 0.2611 & 0.1426 & 0.9442 & 0.1412 \\ 0.1502 & 0.2611 & 0.1412 & 0.9430 \end{bmatrix} \quad (4)$$

$$\mathfrak{R}_{R_{XD}}^{\frac{1}{2}} = \begin{bmatrix} 0.9371 & 0.1460 & 0.2798 & 0.1491 \\ 0.1460 & 0.9375 & 0.1465 & 0.2798 \\ 0.2798 & 0.1465 & 0.9375 & 0.1460 \\ 0.1491 & 0.2798 & 0.1460 & 0.9371 \end{bmatrix} \quad (5)$$

where the subscript  $S, R, D$  stands for Source (Sensor node), Relay, and Destination (Sink node) respectively.

#### 4. MIMO Relaying Channel Capacity

Recall that for WSN application, the propagation channel can be classified as narrowband. So, for a narrowband MIMO system with  $M$  antennas at source node (sensor),  $L$  antennas at relay node, and  $N$  antennas at destination node (sink), the complex baseband representation of the received signal at relay node can be denoted as

$$x(t) = H_1 s(t) + n_1(t) \quad (6)$$

where  $x(t) \in C^L$  is the receive signal vector at relay node,  $s(t) \in C^M$  is the transmitted signal vector from source node,  $H_1 \in C^{L \times M}$  is the channel response matrix between the source (S) and relay node (R), and  $n_1(t) \in C^L$  is the zero-mean additive white Gaussian noise vector between S and R with variance  $\sigma^2$ .

Similarly, the complex equivalent baseband of the received signal at destination node (D) can be denoted as

$$y(t) = H_2 z(t) + n_2(t) \quad (7)$$

where  $y(t) \in C^N$  is the receive signal vector at destination node,  $z(t) = Gx(t) \in C^L$  is the transmitted signal vector from the relay node,  $H_2 \in C^{N \times L}$  is the channel response matrix between the R and D, and  $n_2(t) \in C^N$  is the zero-mean additive white Gaussian noise vector between R and D with variance  $\sigma^2$ . The term  $G$  is a  $L \times L$  linear combining matrix at relay node. It represents the optimal amplifier gain at relay node.

From Eqs. (6) and (7), the received signal at D can be rewritten as

$$\begin{aligned} y(t) &= H_2 G x(t) + n_2(t) \\ &= H_2 G H_1 s(t) + H_2 G n_1(t) + n_2(t) \end{aligned} \quad (8)$$

with

$$H_1 = V_1 \mathfrak{R}_{R_{XR}}^{\frac{1}{2}} U \mathfrak{R}_{T_{XS}}^{\frac{1}{2}} \quad (9)$$

$$H_2 = V_2 \mathfrak{R}_{R_{XD}}^{\frac{1}{2}} U \mathfrak{R}_{T_{XR}}^{\frac{1}{2}} \quad (10)$$

where  $V_1$ , and  $V_2$  are the magnitudes of the received signals corresponding to the channel  $H_1$ , and  $H_2$  respectively. Note that these magnitudes are the linear scaled version of the inverted pathloss because in [11], the pathloss are calculated using 0dBm transmitted power. The first term of Eq. (8) represents the signal whereas the last two terms represent the noise.

Recall that, in [14], the MIMO channel capacity for direct link between S and D is denoted as:

$$C_{Direct} = \log_2 \left[ \det \left[ I_N + \frac{P}{M\sigma^2} H_0 H_0^H \right] \right] \quad (11)$$

with the channel response matrix between the source and destination

$$H_0 = V_0 \mathfrak{R}_{R_{XD}}^{\frac{1}{2}} U \mathfrak{R}_{T_{XS}}^{\frac{1}{2}} \quad (12)$$

where  $\det[\cdot]$  denotes the determinant operator,  $[\cdot]^H$  denotes Hermitian transpose of a matrix,  $I_N$  is an identity matrix of size  $N$ ,  $P$  is total transmitted power at sensor node,  $\sigma^2$  is the total noise power at sink node, and  $V_0$  is the magnitude of the received signal corresponding to the channel  $H_0$ .

In order to evaluate the proposed method mentioned in Sect. 2, a fair comparison between the AF and DF relay schemes must be made.

##### 4.1 Amplify-Forward Relay Scheme

Unlike [10], we model our relay network as a two-phase procedure, i.e. the destination node and relay node receive the signal in different time slots. From [15], we rewrite the MIMO channel capacity formula using the AF relay scheme as:

$$C_{Relay}^{AF} = \frac{1}{2} \log_2 \left[ \det \left[ I_N + \frac{P}{M\sigma^2} H_2 G H_1 H_1^H G^H H_2^H \left( I_N + H_2 G G^H H_2^H \right)^{-1} \right] \right] \quad (13)$$

The factor  $\frac{1}{2}$  comes from the fact that the signal transmitted from the sensor node needs to use two time slots before reaching the sink node. For simplicity we ignore the channel state information (CSI). However, for optimum use of transmitted power at the relay node,  $G$  is chosen in such a way as to retransmit the signal at full power  $P$ .

$$G = \frac{V_{out}}{V_{in}} I_L = \frac{\sqrt{P}}{\sqrt{P_R}} I_L = \sqrt{\frac{P}{P_R}} I_L \quad (14)$$

where  $V_{out}$  and  $V_{in}$  represent the magnitude at the output and input of the amplifier respectively,  $P$  is the total transmitted power at the relay node,  $P_R = P_{Signal} + P_{Noise}$  is the total received power at the relay node, and  $I_L$  is an identity matrix of size  $L$ .

From Eq. (6), the total received power at the relay node

can be rewritten as:

$$P_R = \text{trace} \left[ \frac{P}{M} H_1 H_1^H + \sigma^2 I_L \right] \quad (15)$$

This concept looks similar to [16]. However, in [16], the relay gain is valid for relay nodes with a single antenna only.

Note that  $C_{Relay}^{AF}$  represents the MIMO channel capacity using  $S \rightarrow R \rightarrow D$  path. There are many reasons to choose between direct link and relay link at the sink node to maximize the channel capacity. However, in this method, we are only concerned with the  $C_{Direct}$  and  $C_{Relay}^{AF}$ .

## 4.2 Decode-and-Forward Relay Scheme

In order to make a fair comparison with the AF scheme, we model this relay network as a two-phase procedure, and use  $P$  as the retransmitted power at the relay node.

Since DF relay retransmits the re-encoding version of the received signal, we assume that the relay node can decode correctly the message sent by sensor node. And, Eq. (7) is rewritten as:

$$y(t) = H_2 \tilde{s}(t) + n_2(t) \quad (16)$$

where  $\tilde{s}(t) \in C^L$  is the retransmitted signal vector from the relay node. The MIMO channel capacity between sensor and relay node, and relay and sink node are denoted respectively as:

$$C_{SR} = \log_2 \left[ \det \left[ I_L + \frac{P}{M\sigma^2} H_1 H_1^H \right] \right] \quad (17)$$

$$C_{RD} = \log_2 \left[ \det \left[ I_N + \frac{P}{L\sigma^2} H_2 H_2^H \right] \right] \quad (18)$$

At the sink node, we do not perform any statistical decision as mentioned in [17]. Instead, we will consider the maximum channel capacity that can carry through the  $S \rightarrow R \rightarrow D$  path. Since the relay node retransmits the re-encoded version of the signal sent by the sensor node, and it takes two time slots to reach sink node, the final version of MIMO channel capacity using the DF relay scheme can be denoted as:

$$C_{Relay}^{DF} = \min \left\{ \frac{1}{2} C_{SR}, \frac{1}{2} C_{RD} \right\} \quad (19)$$

## 5. Simplified Version Using Jensen's Inequality

As stated in Sect. 2, the proposed algorithm used to find the optimum position to place relay nodes (so that this system can cover the largest number of sensor nodes) is based on cross-point between the mean (ergodic) channel capacity of the direct link and relay link which uses Monte Carlo method to generate those channel capacities. In this section, we will remove the heavy computational loads imposed by the Monte Carlo method by using Jensen's inequality.

According to the inequality and concavity of  $\log \det$  function [18], we can rewrite Eq. (11) as follows:

$$\begin{aligned} \langle C_{Direct} \rangle &\leq \log_2 \left[ \det \left[ I_N + \frac{P}{M\sigma^2} \langle H_0 H_0^H \rangle \right] \right] \\ &= \log_2 \left[ \det \left[ I_N + \frac{P}{M\sigma^2} \mathfrak{R}_0 \right] \right] \end{aligned} \quad (20)$$

where  $\langle \cdot \rangle$  is the expectation over the channel matrix,  $\mathfrak{R}_0$  defines the correlation matrix at receiver side (sink node) seen from sensor node. For simplicity, we will use this upper-bound of the MIMO ergodic channel capacity in the design and the analysis of the system.

Similarly, with the equality  $\det(I + AB) = \det(I + BA)$ , Eqs. (13), (14), (17), (18), and (19) can be rewritten respectively in a more simple way as below:

$$\langle C_{Relay}^{AF} \rangle \cong \frac{1}{2} \log_2 \left[ \det \left[ I_N + \frac{P}{M\sigma^2} \mathfrak{R}_2 G^2 \mathfrak{R}_1 \left( I_N + \mathfrak{R}_2 G^2 \right)^{-1} \right] \right] \quad (21)$$

$$G \cong \sqrt{\frac{P}{\text{trace} \left[ \frac{P}{M} \mathfrak{R}_1 + \sigma^2 I_L \right]}} I_L \quad (22)$$

$$\langle C_{SR} \rangle \cong \log_2 \left[ \det \left[ I_L + \frac{P}{M\sigma^2} \mathfrak{R}_1 \right] \right] \quad (23)$$

$$\langle C_{RD} \rangle \cong \log_2 \left[ \det \left[ I_N + \frac{P}{L\sigma^2} \mathfrak{R}_2 \right] \right] \quad (24)$$

$$\langle C_{Relay}^{DF} \rangle = \min \left\{ \frac{1}{2} \langle C_{SR} \rangle, \frac{1}{2} \langle C_{RD} \rangle \right\} \quad (25)$$

where  $\mathfrak{R}_1$  and  $\mathfrak{R}_2$  define the correlation matrix at relay node seen from sensor node, and at sink node seen from relay node respectively. Note that the validity of these approximations have been proved by numerical simulation for the design of the relay position with a required channel capacity.

### 5.1 Uncorrelated Channel Matrix

In this case, we suppose that there is no correlation between sub-channels. So, the correlation matrix can be written as:

$$\mathfrak{R}_0 = V_0^2 N I_N \quad (26)$$

$$\mathfrak{R}_1 = V_1^2 L I_L \quad (27)$$

$$\mathfrak{R}_2 = V_2^2 N I_N \quad (28)$$

### 5.2 Correlated Channel Matrix

Since the Kronecker channel model is chosen as stated in Eqs. (9), (10), and (12), the correlation matrix of the corresponding channel can be defined respectively as:

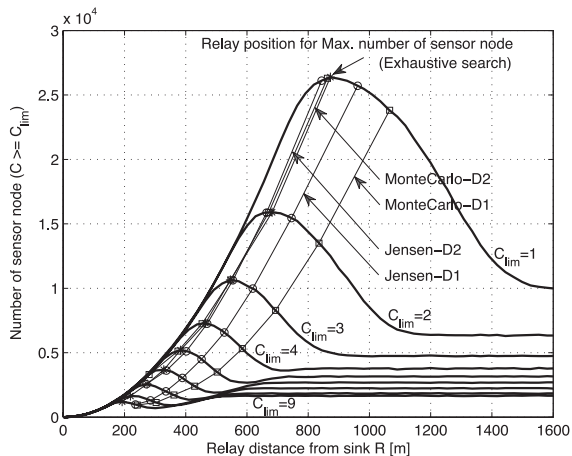
$$\mathfrak{R}_0 = V_0^2 \mathfrak{R}_{RxD} N I_N \quad (29)$$

$$\mathfrak{R}_1 = V_1^2 \mathfrak{R}_{RxR} L I_L \quad (30)$$

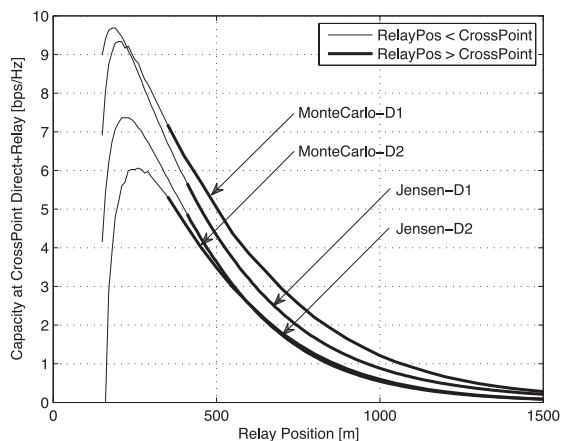
$$\mathfrak{R}_2 = V_2^2 \mathfrak{R}_{RxD} N I_N \quad (31)$$

## 6. Performance Evaluation

In this section, we will first evaluate the validity of the proposed algorithm with different antenna size and then with



(a) Number of sensor node in 7 cells coverage



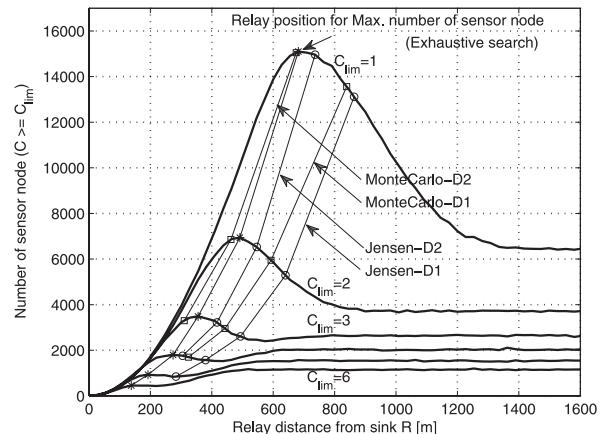
(b) Cross point capacity vs relay position

**Fig. 2**  $4 \times 4$  MIMO, AF relay scheme and iid channel.

the AF relay scheme under the influence of spatial correlation, and with the DF relay scheme under the influence of spatial correlation as well (for fair comparison). In those cases, the comparisons between Monte Carlo and Jensen's inequality are made simultaneously. Finally, we will compare the performance of the system using the AF relay scheme without correlation effect, the AF relay scheme with correlation effect, and the DF relay scheme with correlation effect, by means of relay gain.

Figure 2 shows the number of sensor nodes in the coverage of the system and the channel capacity at the cross-point if the AF is used at the relay nodes and all channel matrices are uncorrelated. In this case, Eqs. (11), (13), and (14) are used to generate the graph called MonteCarlo-D1 and MonteCarlo-D2, whereas Eqs. (20), (21), and (22) along with Eqs. (26), (27), and (28) are used to generate the graph called Jensen-D1 and Jensen-D2.

We can see that both MonteCarlo-D2 and Jensen-D2 provide the results very close to the exhaustive method (optimum results), and that their validity holds for the required channel capacity  $C_{lim}$  up to 6 bps/Hz and 7 bps/Hz respec-

**Fig. 3** Number of sensor node in 7 cells coverage. ( $2 \times 2$  MIMO, AF relay scheme and iid channel)

tively. Note that for  $C_{lim} > 7$  bps/Hz, there is no need to add the relay nodes since only the sink node can provide such a high capacity, thus no need to find the relay position by any methods. We can easily verify this Notice from Fig. 2(a) that at Sink-Relay distance  $\mathcal{R} \cong 220$  m, which corresponds to a first peak for  $C_{lim} = 8$  bps/Hz, the number of sensor nodes given by this position is lower than the number of sensor nodes given by  $\mathcal{R} \geq 600$  m. Since the number of sensor nodes seems to be constant from  $\mathcal{R} \geq 600$  m, which means the number of sensor nodes that satisfies  $C_{lim}$  in 7-cell is the same as that in the sink cell. We can say that from that distance  $\mathcal{R}$ , the relay node capacity is lower than the required channel capacity  $C_{lim}$  and the relay nodes are useless in this condition. Similarly for  $C_{lim} = 9$  bps/Hz. For those reasons, we can say that these two methods are accurate enough to estimate the position to place relay nodes for the largest effective coverage.

For MonteCarlo-D1 and Jensen-D1, the results are different from the exhaustive search and will not be considered in the following discussion. However, we still show these results in the figures as reference only.

Now, let us verify whether these methods are still valid for  $2 \times 2$  MIMO and SISO or not. From Fig. 3, we see that both MonteCarlo-D2 and Jensen-D2 can estimate the optimum relay position. As mentioned above, our objective is to maximize the number of sensor nodes served by the system, so we do not care too much about the differences on distance. So, if the given relay position, estimated by the model, can provide the number of sensor nodes close to the optimum case, we can accept it. From this figure, we can also see that the maximum channel capacity that the relay system can handle decreases from 7 bps/Hz (in  $4 \times 4$  MIMO case, Fig. 2) to only 3 bps/Hz in this case ( $2 \times 2$  MIMO) and to 2 bps/Hz in SISO case (Fig. 4). If the required channel capacity  $C_{lim}$  is higher than 3 bps/Hz, it is useless to add more relay nodes since only the sink node can provide such required capacity, and our estimations are still valid.

Note that the irregularity in the figures is due to the limited repeated computation of the Monte Carlo method. This



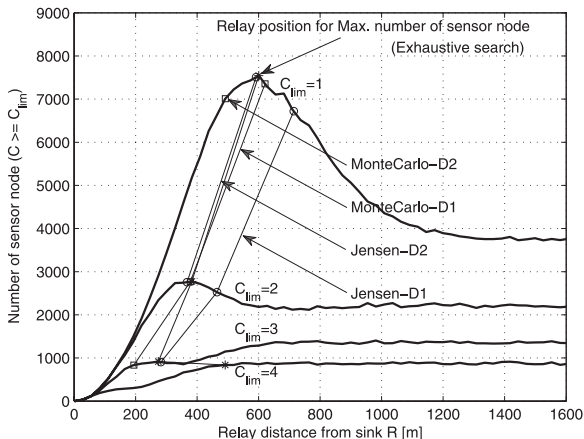


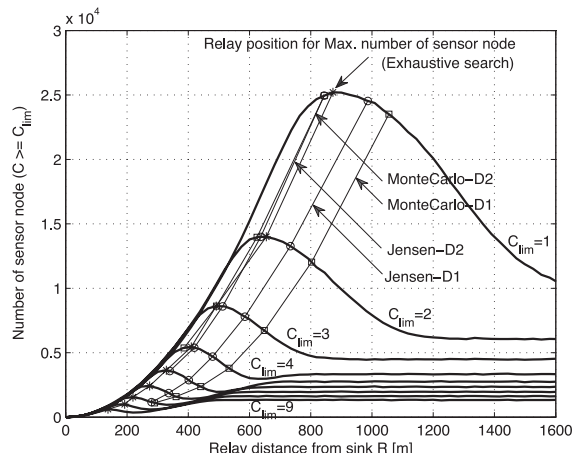
Fig. 4 Number of sensor node in 7 cells coverage. (SISO, AF relay scheme and iid channel)

irregularity can be seen in all figures, especially in Fig. 4 where the number of sensor nodes in the coverage decrease due to the required high channel capacity, with a single antenna at each node. We can overcome this by increasing the repeated computation number of the Monte Carlo method, however, due to limited time, and the result is still acceptable; we ignore this irregularity effect. The reason why the increase of the repeated computation number can overcome the irregularity caused by the decreased number of sensor nodes in the coverage is that the position of sensor nodes are randomly distributed over a given area ( $2 \times 10^5$  sensor nodes in  $5569 \times 5569 \text{ m}^2$ ), so if we can count only a few number of sensor nodes, we should repeat this counting process many times in order to overcome this random characteristic.

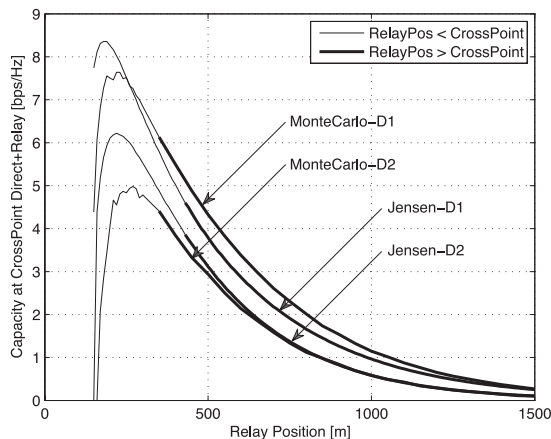
From Fig. 4, we can see that only Jensen-D2 can provide the results close to the optimums and that it can estimate the relay position for a required channel capacity  $C_{lim}$  up to 2 bps/Hz. Over that value, there is no use of relay nodes, so, the ability to predict is not important. For MonteCarlo-D2, it can predict only for  $C_{lim} = 1$  bps/Hz. In this case, Jensen-D2 is a little better than MonteCarlo-D2.

Now, let us see the influence of spatial correlation over our estimation and optimum relay position. Figure 5 shows that the number of sensor nodes in the coverage of the system and the channel capacity at cross-point when AF is used at relay nodes and all channel matrices are correlated. In this case, Eqs. (11), (13), and (14) along with Eqs. (9), (10), and (12) are used to generate the graph called MonteCarlo-D1 and MonteCarlo-D2, whereas Eqs. (20), (21), and (22) along with Eqs. (29), (30), and (31) are used to generate the graph called Jensen-D1 and Jensen-D2.

From this figure, we can see that both MonteCarlo-D2 and Jensen-D2 can still provide the results close to the optimums under the correlation effect. Normally, as mentioned in [19], either receive or transmit bounds alone are not accurate for the whole range of correlation coefficients. However, since the AF relay scheme is used, the correlation effect can be negligible by means of the relay gain  $G$ . We can also conclude that with the AF relay scheme, not only the



(a) Number of sensor node in 7 cells coverage



(b) Cross point capacity vs relay position

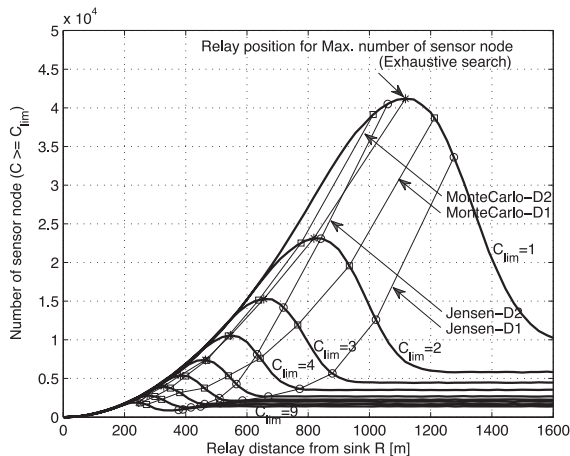
Fig. 5  $4 \times 4$  MIMO, AF relay scheme with spatial correlation effect.

upper-bound effect that can be significantly cancelled out by means of the relay gain  $G$  as shown in Fig. 2, but also the correlation effect (Fig. 5).

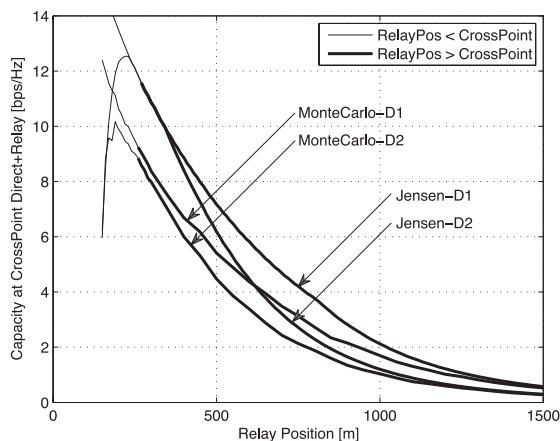
Since the spatial correlation effect will decrease the channel capacity values (both direct and relay links), it also affects the maximum number of sensor nodes served by the system as well. We can see that, in Fig. 2, the maximum number of sensor nodes where  $C_{lim} = 1$  bps/Hz, is about 26500 nodes whereas in Fig. 5, this value is about 25000 nodes only.

In short, this spatial correlation will decrease the effective coverage of the system (has influence on optimum relay position), but not on our estimation.

Now let us evaluate the effect of the relay node scheme over the optimum relay position and its estimation. Figure 6 shows the number of sensor nodes in the coverage of the system and the channel capacity at cross-point if DF is used at the relay node and all channel matrix are correlated. In this case, Eqs. (11), and (19) along with Eqs. (9), (10), and (12) are used to generate the graph called MonteCarlo-D1 and MonteCarlo-D2, whereas Eqs. (20), and (25) along



(a) Number of sensor node in 7 cells coverage



(b) Cross point capacity vs relay position

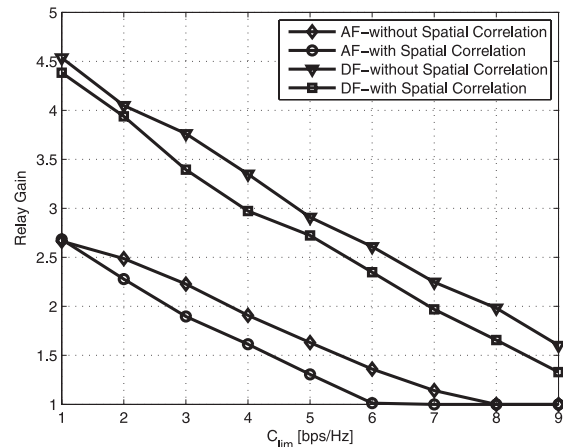
Fig. 6  $4 \times 4$  MIMO, DF relay scheme with spatial correlation effect.

with Eqs. (29), (30), and (31) are used to generate the graph called Jensen-D1 and Jensen-D2.

From Fig. 6, we can see that only MonteCarlo-D2 can provide the results close to the optimums, even if it seems to fail to predict the relay position at  $C_{lim} = 1$  bps/Hz. For Jensen-D2, it can predict only the position of relay nodes where  $C_{lim} < 4$  bps/Hz, and fail to predict the rest ( $C_{lim} > 3$  bps/Hz). By using DF at the relay nodes; the effect of spatial correlation can be seen clearly at high SNR. This is because at high SNR, the second term in the det is dominant over the first term ( $I_L$  or  $I_N$ ). See Eqs. (20), (23) and (24).

By using the DF scheme at the relay nodes, the relay system can handle the required channel  $C_{lim}$  up to 9 bps/Hz and the maximum number of sensor nodes served by the system also increase remarkably from about 25000 nodes (AF and spatial correlation case) to 41500 nodes in this case (DF and spatial correlation).

In order to see the difference between each case more clearly, we plot all the relay gain of each system, including DF with uncorrelated channel, in Fig. 7. From this figure, we can see that by using DF scheme at relay nodes, the relay

Fig. 7 Relay gain vs  $C_{lim}$  in  $4 \times 4$  MIMO case.

gain at  $C_{lim} = 1$  bps/Hz can be increased from about 2.67 in AF case, to about 4.5 in DF case. Moreover, by using the DF relay scheme, the relay system can handle the required channel capacity up to 9 bps/Hz, which is unrealized with AF scheme (only handle  $C_{lim}$  up to 5 bps/Hz).

We can also see the effect of spatial correlation over the performance of the system from this figure. Without spatial correlation, the system that uses AF scheme can handle the  $C_{lim}$  up to 7 bps/Hz, but when adding the spatial correlation effect to the system, the performance decreases to 5 bps/Hz. Similar effect can be seen in the DF scheme. However, this spatial correlation can only effect the performance of the system at high required channel capacity only which corresponds to high SNR.

## 7. Conclusion

From the performance analysis in Sect. 5, we draw the conclusions listed below:

- The optimum relay position changes under spatial correlation effect and relay scheme as shown in Fig. 2, Fig. 5, and Fig. 6.
- The effect of spatial correlation over our estimation can be seen at high SNR or high required channel capacity  $C_{lim}$  only, although this affects the optimum relay position and the total number of sensor nodes served by the system in all required  $C_{lim}$ .
- For the same transmitted power at relay node, DF relay scheme can provide broader coverage than AF relay scheme with or without spatial correlation effect.
- In all cases ( $4 \times 4$  MIMO,  $2 \times 2$  MIMO, SISO, Correlated channel, or Uncorrelated channel), MonteCarlo-D2 can be considered as the most reliable estimator to find the optimum relay position.
- For DF relay scheme, if the required channel capacity is low ( $C_{lim} < 4$  bps/Hz), Jensen-D2 can be used since this method provides an acceptable result and has low computational load (direct calculation).
- If the AF relay scheme is chosen, Jensen-D2 can be



used to provide the good results as MonteCarlo-D2.

We can conclude that the performance of the predictor MonteCarlo-D2 compensates with its computational capacity required comparing to Jensen-D2. However, MonteCarlo-D2 is still much lighter than the conventional exhaustive search.

## References

- [1] A.F. Molisch, *Wireless Communications*, John Wiley & Sons, IEEE Press, 2005.
- [2] J. Tang, B. Hao, and A. Sen, "Relay node placement in large scale wireless sensor networks," *Comput. Commun.*, vol.29, pp.490–501, 2006.
- [3] A. Kashyap, S. Khuller, and M. Shayman, "Relay placement for higher order connectivity in wireless sensor networks," *INFOCOM 2006, 25th IEEE International Conference on Computer Communications*, pp.1–12, April 2006.
- [4] X. Cheng, D.Z. Du, L. Wang, and B. Xu, "Relay sensor placement in wireless sensor networks," *Wirel. Netw.*, vol.14, pp.347–355, 2008.
- [5] J. Suomela, "Approximating relay placement in sensor networks," *3rd ACM International Workshop on Performance Evaluation of Wireless Ad Hoc, Sensor and Ubiquitous Networks*, pp.145–148, Torremolinos, Spain, Oct. 2006.
- [6] E. Falck, P. Floréen, P. Kaski, J. Kohonen, and P. Orponen, "Balanced data gathering in energy-constrained sensor networks," *AL-GOSENSORS 2004, Turku, LNCS 3121*, pp.59–70, 2004.
- [7] P. Floréen, P. Kaski, J. Kohonen, and P. Orponen, "Exact and approximate balanced data gathering in energy-constrained sensor networks," *Theor. Comput. Sci.*, vol.344, pp.30–46, Nov. 2005.
- [8] A. Giorgetti, M. Chiani, M. Shafi, and P.J. Smith, "Characterizing MIMO capacity under the influence of spatial/temporal correlation," *Proc. Australian Commun. Theory Workshop, AusCTW 2003, Melbourne, Australia, Feb. 2003*.
- [9] T.D. Abhayapala, R.A. Kenney, and J.T.Y. Ho, "On capacity of multi-antenna wireless channels: Effects of antenna separation and spatial correlation," *Proc. 3rd AusCTW, 2002*.
- [10] G. Li and H. Liu, "On the capacity of broadband relay networks," *Signals, Systems and Computers, IEEE Conference Record'38*, vol.2, pp.1318–1322, Nov. 2004.
- [11] K. Leng, K. Sakaguchi, and K. Araki, "Pathloss model for factory environment," *ISMAL Conference, Bangkok, Thailand, Jan. 2009*.
- [12] M. Otani, H. Harada, and R. Funada, "A UHF (950 MHz) band RFID reader compliant with Japanese radio law," *IEEE Industrial Electronics, IECON 2006 — 32nd Annual Conference*, pp.4773–4778, Nov. 2006.
- [13] C. Oestges, "Validity of the Kronecker model for MIMO correlated channels," *IEEE 63rd, VTC 2006-Spring*, pp.2818–2822, 2006.
- [14] I.E. Telatar, "Capacity of multi-antenna Gaussian channels," *Euro. Trans. Telecommun.*, vol.1, no.6, pp.585–595, Nov./Dec. 1999.
- [15] O. Muñoz, J. Vidal, and A. Agustin, "Non-regenerative MIMO relaying with channel state information," *ICASSP'05. IEEE International Conference*, vol.3, pp.iii/361–iii/364, March 2005.
- [16] J.Y. Jung, "On the performance of cooperative diversity in infrastructure-based networks with two relays," *IFIP Networking 2006, LNCS 3976*, pp.1138–1143, 2006.
- [17] R. Rajagopalan, D. Reynolds, and B.D. Woerner, "Performance of cooperative diversity using MIMO systems," *Proc. 2006 16th Annual Wireless Symposium (MPRG'06)*, 2006.
- [18] T.M. Cover and J.A. Thomas, *Elements of Information Theory*, John Wiley & Sons, New York, 1991.
- [19] S. Loyka and A. Kouki, "On the use of Jensen's inequality for MIMO channel capacity estimation," *Canadian Conf. on Electrical and Computer Engineering (CCECE 2001)*, pp.475–480, Toronto, Canada, May 2001.



communication system, electronic and computer programming.

**KY Leng** was born in Battambang, Cambodia, on May 06, 1979. He received a B.E. degree in electrical engineering from the Institute of Technology of Cambodia, in 2001, and M.E. degree in electrical engineering from the Chulalongkorn University, Bangkok, Thailand in 2005. In 2001–2003 and 2005–2006, he was a lecturer at the Institute of Technology of Cambodia. From 2006 till now, he is a Ph.D. student at the Tokyo Institute of Technology, Tokyo, Japan. His research interests are communi-



IEEE AP-S Japan chapter in 2001 and 2002 respectively, the Outstanding Paper Award from SDR Forum in 2004 and 2005 respectively, and the Excellent Paper Award from IEICE Japan in 2005. His current research interests are in MIMO propagation measurement, MIMO communication system, and software defined radio. He is a member of IEEE.

**Kei Sakaguchi** was born in Osaka, Japan, on November 27, 1973. He received a B.E. degree in electrical and computer engineering from the Nagoya Institute of Technology, Japan, in 1996, and a M.E. degree in information processing from the Tokyo Institute of Technology, in 1998. In 2000–2007, he was an Assistant Professor at the Tokyo Institute of Technology. He is currently an Associate Professor at the Tokyo Institute of Technology. He received the Young Engineer Awards both from IEICE Japan and



the University of Texa, Austin and University of Illinois, Urbana, respectively. He is currently a Professor at the Tokyo Institute of Technology. His research interests are information security, coding theory, communication theory, circuit theory, electromagnetic theory, and microwave circuits, etc. He is a member of IEEE and Information Processing Society of Japan.

**Kiyomichi Araki** was born in Nagasaki on January 7, 1949. He received a B.E. degree in electrical engineering from Saitama University, in 1971, and M.E. and Ph.D. degrees in physical electronics both from the Tokyo Institute of Technology, in 1973 and 1978, respectively. In 1973–1975, and 1978–1985, he was a Research Associate at the Tokyo Institute of Technology, and in 1985–1995 he was an Associate Professor at Saitama University. In 1979–1980 and 1993–1994 he was a visiting research scholar at